Heavy ions and parton saturation from RHIC to LHC

A. Dainese
INFN - Laboratori Nazionali di Legnaro, Legnaro (Padova), Italy

Abstract
The phenomenology of gluon saturation at small parton momentum fraction, Bjorken-x, in the proton and in the nucleus is introduced. The experimentally-accessible kinematic domains at the nucleus–nucleus colliders RHIC and LHC are discussed. Finally, the saturation hints emerging from measurements at RHIC and the perspectives for LHC are described.

1 Introduction: small-x gluons in the proton and in the nucleus

In the collinear factorization approach of perturbative QCD, the parton distribution functions (PDFs) of the proton are determined through global fits obtained using the DGLAP scale evolution equations [1–3]. The HERA ep deep inelastic scattering (DIS) data on the proton structure function $F_2(x,Q^2)$ as a function of the parton momentum fraction Bjorken-x and of the squared momentum transfer Q^2, and, especially, the Q^2 slope, $\partial F_2(x,Q^2)/\partial \ln Q^2$, in the small-$x$, $3\times10^{-5} \lesssim x \lesssim 5\times10^{-3}$, and small-$Q^2$ region, $1.5 \lesssim Q^2 \lesssim 10$ GeV^2, set rather stringent constraints on the small-x gluon distribution $xg(x,Q^2)$. In this kinematic region, the gluon distribution exhibits a strong rise towards low x and the agreement of the global fits with the HERA $F_2(x,Q^2)$ data is not as good as it is at larger values of x and Q^2 [4]. In particular, the gluon density xg tends to rise faster than what suggested by the data. This is due to the fact that the kernels of the DGLAP equations only describe splitting of one parton into two or more, so that the resulting evolution is linear in the PDFs. At low Q^2, the small-x gluon density may increase to the point where gluon fusion, $\mathrm{gg}\to\mathrm{g}$, becomes significant. Within the DGLAP framework, this phenomenology can be accounted for in an effective way by including nonlinear corrections in the evolution equations, that is, negative terms of order $\mathcal{O}(g^2)$, $\mathcal{O}(g^3)$, etc... that tame the evolution towards small x. The first nonlinear corrections, the GLRMQ terms, were derived in Ref. [5,6]. A more accurate description of the small-x nonlinearities is achieved in the framework of k_t-factorization, in which the BK equation [7, 8] is used to evolve the PDFs as a function of x for fixed transverse momentum squared, k_t^2, of the gluon. Both approaches to nonlinear gluon dynamics, in DGLAP and in BK, suggest that one can expected potentially-measurable effects in pp collisions at LHC energy, for example in heavy-flavour production [9].

In the case of proton–nucleus and nucleus–nucleus collisions, where nuclei with large mass number A are involved, the nonlinear effects are enhanced by the larger density of gluons per unit transverse area of the colliding nuclei. The high density of gluons at small x and small Q^2 induces a suppression of the observed hard scattering yields with respect to expectations based on a scaling with the number of binary nucleon–nucleon collisions. This reduction affects the kinematic region dominated by small-x gluons: low transverse momentum p_t and forward rapidity y, since, at leading order, we have $x \sim p_\mathrm{t}\exp(-y)/\sqrt{s_\mathrm{NN}}$. The effect, indicated as nuclear shadowing, is usually accounted for in terms of a modification of the parton distribution

functions of the nucleon in the nucleus, $f_i^{\rm A}(x,Q^2)$, with respect to those of the free nucleon, $f_i^{\rm N}(x,Q^2)$:

$$R_i^{\rm A}(x,Q^2) = \frac{f_i^{\rm A}(x,Q^2)}{f_i^{\rm N}(x,Q^2)} \tag{1}$$

where $i = {\rm q_v},\ {\rm q_{sea}},\ {\rm g}$ for valence quarks, sea quarks, and gluons. We have shadowing, $R_{\rm g}^{\rm A} < 1$, for $x \lesssim 5 \times 10^{-2}$. However, as we will discuss in the following, the strength of the reduction is constrained by existing experimental data only for $x \gtrsim 10^{-3}$.

The use of nuclear-modified parton distribution functions allows high-density effects at small x to be accounted for within the framework of perturbative QCD collinear factorization. However, factorization is expected to break down when the gluon phase-space becomes *saturated*. In these conditions, in the collision with an incoming projectile parton, the partons in the target nuclear wave function at small x would act coherently, not independently as assumed with factorization. In the limit, they may form a Colour Glass Condensate (CGC) [10]: a system, that can be describe in analogy to a spin glass, where gluons (colour charges) have large occupation number, as in a condensate. The relevant parameter in the CGC is the so-called saturation scale $Q_{\rm S}^2$, defined as the scale at which the transverse area of the nucleus is completely saturated and gluons start to overlap. This happens when the number of gluons, $\sim {\rm A}\, xg(x,Q_{\rm S}^2)$, multiplied by the typical gluon size, $\sim 1/Q_{\rm S}^2$, is equal to the transverse area, $\sim \pi R_{\rm A}^2$. Thus:

$$Q_{\rm S}^2 \sim \frac{{\rm A}\, xg(x,Q_{\rm S}^2)}{\pi R_{\rm A}^2} \sim \frac{{\rm A}\, xg(x,Q_{\rm S}^2)}{{\rm A}^{2/3}} \sim {\rm A}^{1/3} x^{-\lambda} \sim {\rm A}^{1/3} (\sqrt{s_{\rm NN}})^{\lambda} e^{\lambda y}\,, \quad \text{with } \lambda \approx 0.3. \tag{2}$$

$Q_{\rm S}^2$ grows at forward rapidity, at high c.m.s. energy , and it is enhanced by a factor about 6 ($200^{1/3}$) in the Au or Pb nucleus, with respect to the proton. Saturation affects the processes in the region $Q^2 \lesssim Q_{\rm S}^2$, where gluon recombination dominates and factorization may start to become invalid.

2 Exploring the saturation region

Figure 1, elaborated from Ref. [11], shows the experimental acceptances in the plane (x,Q^2) for: the nuclear DIS (lepton–nucleus) experiments NMC, SLAC-E139, FNAL-E665, EMC; the nuclear Drell-Yan (lepton–nucleus) experiment FNAL-E772; the RHIC (dAu) experiments BRAHMS and PHENIX; the experiments in preparation at LHC, ALICE, ATLAS, CMS, LHCb.

The current knowledge of the nuclear modification of the PDFs is based on the nuclear DIS data, reaching down to $x \gtrsim 10^{-3}$. As it can be seen from the figure, the LHC will give access to an unexplored small-x domain of QCD. There are several model extrapolations of the amount of nuclear shadowing in this region, with $R_g^{\rm Pb}(x,Q^2)$ ranging from 0.1 to 0.8 at $x \sim 10^{-4}$ and $Q^2 \sim 2\ {\rm GeV}^2$ (see e.g. Ref. [12]).

The estimated values of the saturation scale in heavy-ion collisions at RHIC and LHC are reported in the figure. For a Au nucleus probed at RHIC energy, $\sqrt{s_{\rm NN}} = 200\ {\rm GeV}$, the estimated saturation scale is $Q_{\rm S}^2 \sim 2\ {\rm GeV}^2$: processes that involve gluons at $x < 10^{-3}$–10^{-2} are affected. For a Pb nucleus probed at LHC energy, $\sqrt{s_{\rm NN}} = 5.5\ {\rm TeV}$, the estimated saturation scale is $Q_{\rm S}^2 \sim 5\ {\rm GeV}^2$: processes that involve gluons at $x < 10^{-4}$–10^{-3} are affected. The line at $Q^2 = 1\ {\rm GeV}^2$

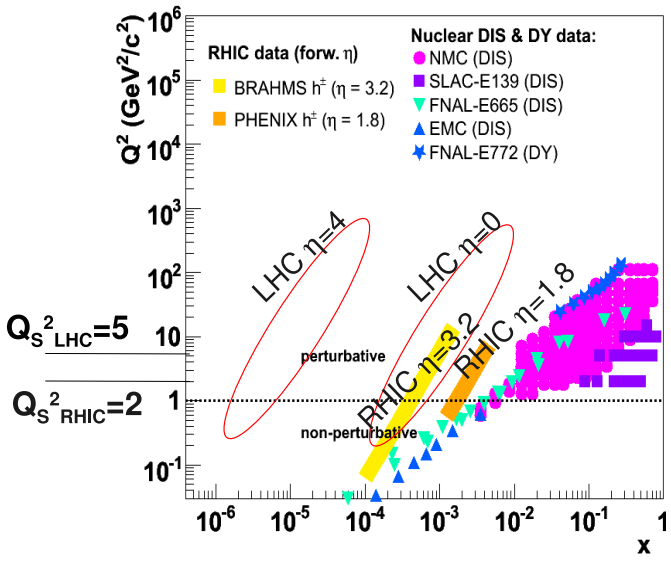

Fig. 1: The kinematic regions in x and Q^2 explored by nuclear DIS and Drell-Yan experiments, by RHIC experiments, and by experiments in preparation at LHC. Elaborated from a compilation in Ref. [11].

shows the lower limit of applicability of the perturbative QCD approach. At variance from RHIC, where the perturbative region and the saturation region have little overlap, at the LHC it will be possible to explore the saturation region with perturbative probes, like heavy quarks, and $\mathrm{c\overline{c}}$ in particular. This means that discrepancies between charm production measurements close to the threshold and perturbative predictions could signal the onset of saturation effects. We will further discuss this point in Section 4.2. Another very promising approach to the investigation of small-x effects is by measuring hard process (jets, heavy quarks, weak-interaction vector bosons) in the forward rapidity region (see Section 4.1).

3 Hints of saturation at RHIC

Two experimental observations in heavy-ion collisions at RHIC support the saturation predictions of a reduced parton flux in the incoming ions due to nonlinear QCD effects. On one hand, the measured hadron multiplicities (see e.g. Ref. [13]), $\mathrm{d}N_{\mathrm{ch}}/\mathrm{d}\eta \approx 700$, are significantly lower than the $\mathrm{d}N_{\mathrm{ch}}/\mathrm{d}\eta \approx 1000$ values predicted by minijet [14] or Regge [15] models, but are well reproduced by CGC approaches [16]. Assuming parton–hadron duality, hadron multiplicities at mid-rapidity rise proportionally to Q_{S}^2 times the transverse (overlap) area [17], a feature that accounts naturally for the experimentally-observed factorization of $\sqrt{s_{\mathrm{NN}}}$- and centrality-dependences in $\mathrm{d}N_{\mathrm{ch}}/\mathrm{d}\eta$ (Fig. 2, left). The second possible manifestation of CGC-like effects in the RHIC data is the BRAHMS observation [18] of suppressed yields of semi-hard hadrons ($p_{\mathrm{t}} \approx$ 2–4 GeV/c) in dAu relative to pp collisions at forward rapidities (up to $\eta \approx 3.2$, Fig. 2, right). Hadron production at such small angles is sensitive to partons in the Au nucleus with $x^{\mathrm{min}} \sim p_{\mathrm{t}} \exp(-\eta)/\sqrt{s_{\mathrm{NN}}} \sim 10^{-3}$ [19]. The observed nuclear modification factor, $R_{\mathrm{dAu}} \approx$

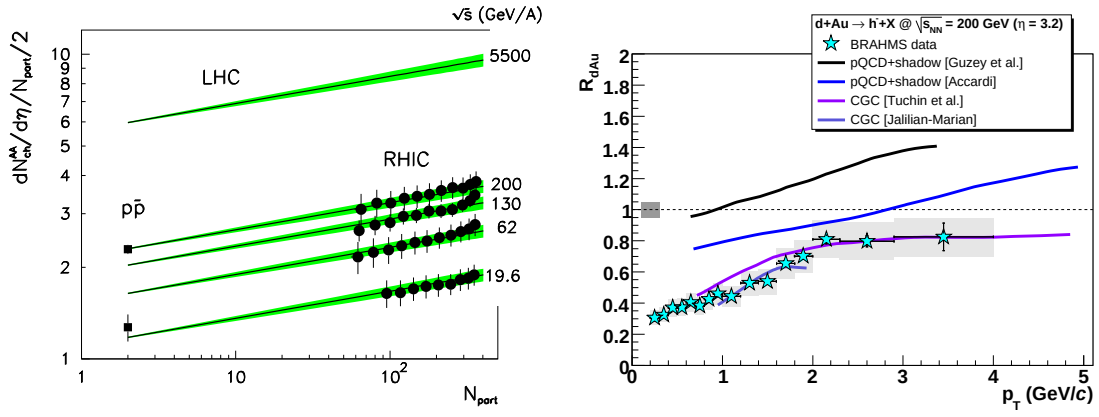

Fig. 2: Hints of saturation at RHIC. Left: Normalized $\mathrm{d}N_{\mathrm{ch}}/\mathrm{d}\eta$ as a function of c.m.s. energy and centrality (given in terms of the number of nucleons participating in the collision, N_{part}) measured by PHOBOS in Au–Au [13] compared with saturation predictions [17]. Right: Nuclear modification factor $R_{\mathrm{dAu}}(p_{\mathrm{t}})$ for negative hadrons at η = 3.2 in dAu at $\sqrt{s_{\mathrm{NN}}}$ = 200 GeV: BRAHMS data [18] compared to pQCD [19, 20] and CGC [21, 22] predictions.

0.8, cannot be reproduced by pQCD calculations [19, 20] that include the same nuclear shadowing that describes the dAu data at $\eta = 0$, but can be described by CGC approaches that parametrise the Au nucleus as a saturated gluon wavefunction [21, 22].

4 Perspectives for LHC

4.1 Accessing the small-x region with hard processes at forward rapidity

The four LHC experiments —i.e. the two general-purpose and high-luminosity ATLAS and CMS detector systems as well as the heavy-ion-dedicated ALICE and the heavy-flavour-oriented LHCb experiments— have all detection capabilities in the forward direction very well adapted for the study of low-x QCD phenomena with hard processes in collisions with proton and ion beams (see e.g. Ref. [23] for more details):

- Both CMS and ATLAS feature hadronic calorimeters in the range $3< |\eta| <5$ which allow them to measure jet cross-sections at very forward rapidities. Both experiments feature also zero-degree calorimeters (ZDC, $|\eta| \gtrsim 8.5$ for neutrals), which are a basic tool for neutron-tagging "ultra-peripheral" Pb–Pb photoproduction interactions. CMS has an additional electromagnetic/hadronic calorimeter (CASTOR, $5.3 < |\eta| < 6.7$) and shares the interaction point with the TOTEM experiment providing two extra trackers at very forward rapidities (T1, $3.1 < |\eta| < 4.7$, and T2, $5.5 < |\eta| < 6.6$) well-suited for DY measurements.
- The ALICE forward muon spectrometer at $2.5 < \eta < 4$, can reconstruct J/ψ and Υ (as well as Z^0) in the di-muon channel, as well as statistically measure single inclusive heavy-quark production via semi-leptonic (muon) decays. ALICE counts also on ZDCs in both sides of the interaction point for forward neutron triggering of Pb–Pb photoproduction

processes.

- LHCb is a single-arm spectrometer covering rapidities $1.8 < \eta < 4.9$, with very good particle identification capabilities designed to accurately reconstruct charm and beauty hadrons. The detector is also well-suited to measure jets, $Q\overline{Q}$ and $Z^0 \to \mu\mu$ production in the forward hemisphere.

4.2 Probing small-x gluons with heavy quarks

As already mentioned, at LHC it will be possible to probe the saturation region with perturbative probes, such as heavy quarks. The x regime relevant for charm production in heavy-ion collisions at LHC ($x \gtrsim 2m_{\rm c}\exp(-y)/\sqrt{s_{\rm NN}}$) extends down to $x \sim 10^{-4}$ already at central rapidity $y = 0$ and down to $x \sim 10^{-6}$ at forward rapidity $y \approx 4$ [24]. Charm (and beauty) production cross sections at small $p_{\rm t}$ and forward rapidity are thus expected to be significantly affected by parton dynamics in the small-x region. As an example, the EKS98 parametrisation [25] of the PDFs nuclear modification, shown in Fig. 3 (centre) for $Q^2 = 5\ {\rm GeV}^2$, predicts a reduction of the charm (beauty) cross section at NLO of about 35% (20%) in Pb–Pb at 5.5 TeV and 15% (10%) in pPb at 8.8 TeV [24].

The comparison of heavy-quark production in pp and pPb collisions (where final-state effects, such as parton energy loss, are not expected to be present) is regarded as a sensitive tool to probe nuclear PDFs at LHC energy. The ratio of invariant-mass spectra of dileptons from heavy-quark decays in pPb and pp collisions would measure the nuclear modification $R_{\rm g}^{\rm Pb}$ [26]. Another promising observable in this respect is the nuclear modification factor of the D meson $p_{\rm t}$ distribution, defined as:

$$R^{\rm D}_{\rm pA(AA)}(p_{\rm t},\eta) = \frac{1}{\langle N_{\rm coll}\rangle} \times \frac{{\rm d}^2N^{\rm D}_{\rm pA(AA)}/{\rm d}p_{\rm t}{\rm d}\eta}{{\rm d}^2N^{\rm D}_{\rm pp}/{\rm d}p_{\rm t}{\rm d}\eta}\,. \tag{3}$$

In Fig. 3 (right) we show the sensitivity of $R^{\rm D}_{\rm pPb}$ to different shadowing scenarios, obtained by varying the modification of the PDFs in the Pb nucleus (displayed, for gluons, by the curves labeled 'a', 'b', 'c' and 'EKS98' in the left panel of the same figure). The ALICE experiment will be able to measure D meson production down to almost zero transverse momentum, at central rapidity [27]. As shown by the projected experimental uncertainties on the $\rm D^0$ nuclear modification factor in pPb, reported in the left panel of Fig. 3, this measurement is expected to be sensitive to the level of nuclear shadowing at LHC.

Charmonium production at low $p_{\rm t}$ and forward rapidity is another promising probe of small-x gluons at LHC. All four LHC experiments are expected to have good capability for J/ψ reconstruction in the central and in the forward rapidity region. In particular, ALICE will provide a measurement via di-muons in $2.5 < y < 4$ down to $p_{\rm t} \approx 0$ [27], which probes the poorly-known region $x < 10^{-5}$ where current PDF parametrisations have large uncertainties. Figure 4 shows the J/ψ rapity-differential cross section at NLO from the Color Evaporation Model [30], in $2.5 < y < 4$ with different PDF sets, compared to the projected precision of the ALICE measurement [29].

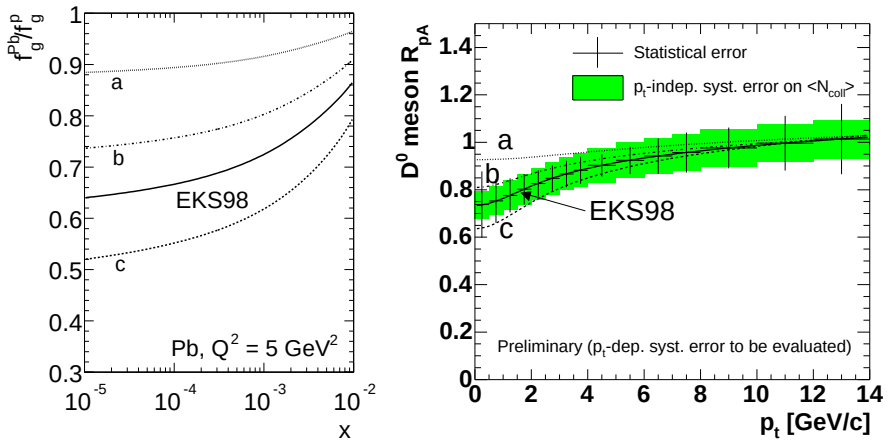

Fig. 3: Charm production in p–Pb at LHC. Left: EKS98 [25] parametrisation for the modification of the gluon PDF in a Pb nucleus at $Q^2 = 5\ \mathrm{GeV}^2 \simeq 4\,m_c^2$, along with three other different scenarios. Right: corresponding $R_{\mathrm{pA}}^{\mathrm{D}}$ in p–Pb at $\sqrt{s_{\mathrm{NN}}} = 8.8$ TeV and expected sensitivity of the ALICE experiment with the $\mathrm{D}^0 \to \mathrm{K}^-\pi^+$ measurement at central rapidity ($|\eta| < 0.9$), with one year of data taking at nominal LHC luminosity [28].

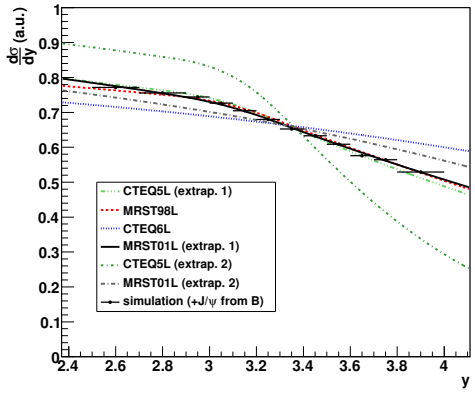

Fig. 4: J/ψ production in pp at LHC. Cross section as a function of rapidity as predicted using different PDF sets (details in the text) , compared to the projected precision of the measurement of the ALICE experiment [29].

.

5 Summary

We have discussed how gluons nonlinear evolution and the phenomenology of saturation are expected to set on at small x in the hadrons, and how these effects are enhanced by the higher transverse gluon density in large nuclei. The study of this almost unexplored regime can provide fundamental insight on the high-energy limit of QCD. We have described the experimental indications of the onset of saturation in heavy-ion collisions at RHIC. The LHC, as a heavy-ion collider, will be a unique laboratory for the investigation of the saturation regime with perturba-

tive probes, such as forward rapidity hard processes and heavy quarks at low momentum and/or forward rapidity.

Acknowledgements: I am grateful to the organizers of the International Symposium on Multiparticle Dynamics 2008 for the invitation and support. I warmly thank D. d'Enterria for stimulating discussions and for providing useful material for the preparation of this contribution, and K. Kutak for valuable comments on the manuscript.

References

[1] Y. L. Dokshitzer, Sov. Phys. JETP **46**, 641 (1977).

[2] V. N. Gribov and L. N. Lipatov, Sov. J. Nucl. Phys. **15**, 438 (1972).

[3] G. Altarelli and G. Parisi, Nucl. Phys. **B126**, 298 (1977).

[4] A. D. Martin, R. G. Roberts, W. J. Stirling, and R. S. Thorne, Eur. Phys. J. **C35**, 325 (2004).

[5] L. V. Gribov, E. M. Levin, and M. G. Ryskin, Nucl. Phys. **B188**, 555 (1981).

[6] A. H. Mueller and J.-w. Qiu, Nucl. Phys. **B268**, 427 (1986).

[7] I. Balitsky, Nucl. Phys. **B463**, 99 (1996).

[8] Y. Kovchegov, Phys. Rev. **D60**, 034008 (1999).

[9] J. Baines *et al.* (2006). hep-ph/0601164.

[10] E. Iancu and R. Venugopalan, World Scientific, Singapore. hep-ph/0303204.

[11] D. G. d'Enterria, Eur. Phys. J. **A31**, 816 (2007). hep-ex/0610061.

[12] K. J. Eskola, H. Paukkunen, and C. A. Salgado, JHEP **07**, 102 (2008). 0802.0139.

[13] B. B. Back *et al.*, Nucl. Phys. **A757**, 28 (2005). nucl-ex/0410022.

[14] M. Gyulassy and X.-N. Wang, Comput. Phys. Commun. **83**, 307 (1994). nucl-th/9502021.

[15] A. Capella, U. Sukhatme, C.-I. Tan, and J. Tran Thanh Van, Phys. Rept. **236**, 225 (1994).

[16] L. D. McLerran and R. Venugopalan, Phys. Rev. **D50**, 2225 (1994). hep-ph/9402335.

[17] N. Armesto, C. A. Salgado, and U. A. Wiedemann, Phys. Rev. Lett. **94**, 022002 (2005). hep-ph/0407018.

[18] I. Arsene *et al.*, Nucl. Phys. **A757**, 1 (2005). nucl-ex/0410020.

[19] V. Guzey, M. Strikman, and W. Vogelsang, Phys. Lett. **B603**, 173 (2004). hep-ph/0407201.

[20] A. Accardi, Acta Phys. Hung. **A22**, 289 (2005). nucl-th/0405046.

[21] D. Kharzeev, Y. Kovchegov, and K. Tuchin, Phys. Lett. **B599**, 23 (2004).

[22] J. Jalilian-Marian, Nucl. Phys. **A748**, 664 (2005). nucl-th/0402080.

[23] D. G. d'Enterria (2008). arXiv:0806.0883.

[24] N. Carrer and A. Dainese (2003). hep-ph/0311225.

[25] K. J. Eskola, V. J. Kolhinen, and C. A. Salgado, Eur. Phys. J. **C9**, 61 (1999). hep-ph/9807297.

[26] A. Accardi *et al.* (2004). hep-ph/0308248.

[27] B. Alessandro *et al.*, J. Phys. **G32**, 1295 (2006).

[28] R. Grosso, PhD Thesis, Università di Trieste (2004).

[29] D. Stocco, PhD Thesis, Università di Torino (2008).

[30] M. Bedjidian *et al.* (2003). hep-ph/0311048.